0273-2289/04/118/0253/$25.00

Structural Analysis of Mycobacterial Lipoglycans

Jérôme Nigou,* Martine Gilleron, Thérèse Brando, and Germain Puzo

Department of Molecular Mechanisms of Mycobacterial Infections, Institut de Pharmacologie et de Biologie Structurale, CNRS UMR 5089, 205, Route de Narbonne, 31077 Toulouse Cedex 4, France, E-mail: jerome.nigou@ipbs.fr

Received May 18, 2003; Revised July 3, 2003; Accepted July 31, 2003

Abstract

Mycobacterium tuberculosis, the causative agent of tuberculosis, is one of the most effective human pathogens. The mycobacterial cell envelope contains lipoglycans, and of particular interest is lipoarabinomannan (LAM), one of the most potent mycobacterial immunomodulatory molecules. The importance of lipoarabinomannan (LAM) in the immunopathogenesis of tuberculosis has incited structural studies on this molecule to (1) establish a precise structural model of the molecule and (2) decipher the structure/function relationships. In recent years, we have focused on the two domains essential for LAM biologic activities: the mannosyl-phosphatidyl-*myo*-inositol anchor and the caps. We review here the recent procedures developed for the structural analysis of these domains.

Index Entries: Mycobacterium; lipoglycan; lipoarabinomannan; structure; capillary electrophoresis; nuclear magnetic resonance.

Introduction

Lipoarabinomannans (LAMs) are lipoglycans ubiquitously found in the cell wall of mycobacteria *(1–6)*. Mycobacteria are acid-fast Gram-positive bacteria and are responsible for different diseases. Among them, *Mycobacterium tuberculosis*, the causative agent of tuberculosis, is one of the most effective human pathogens. LAMs appear as the most potent nonpeptidic mycobacterial molecules that modulate the host immune response *(2,5,7)*. They are amphipathic molecules presenting a tripartite

*Author to whom all correspondence and reprint requests should be addressed.

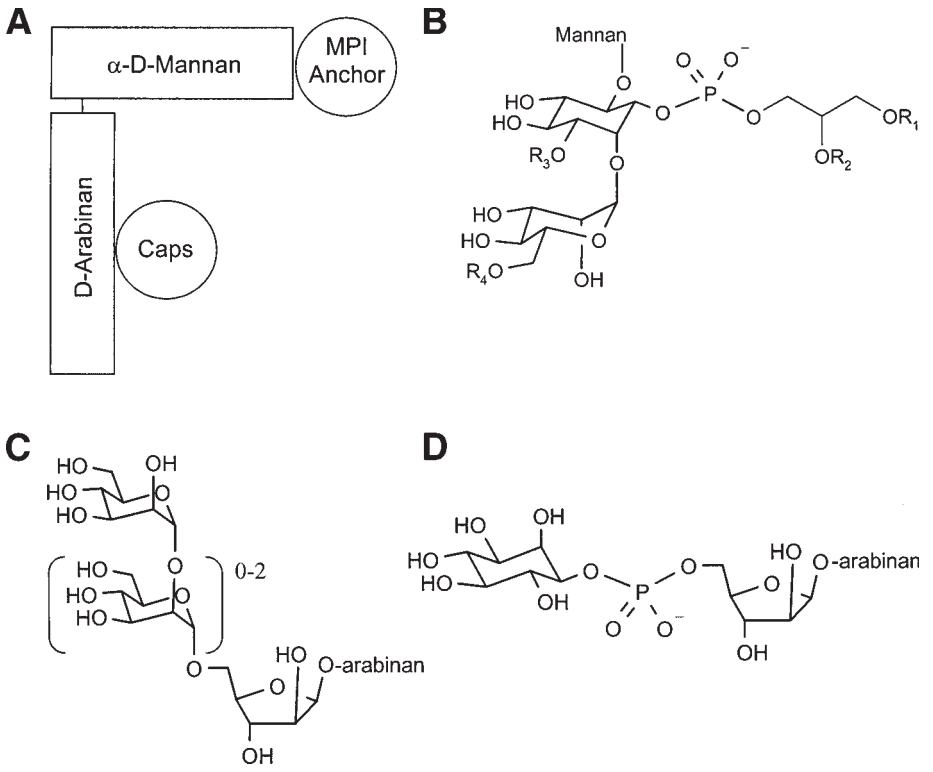

Fig. 1. LAM structural model showing **(A)** an overview and detailed structures of **(B)** the MPI anchor, **(C)** mannooligosaccharide and **(D)** phosphoinositide caps. (B) R_n = fatty acyl groups, mainly palmitic and tuberculostearic acids with stearic acid in a smaller amount.

structure (Fig. 1A) including a mannosyl-phosphatidyl-*myo*-inositol (MPI) anchor (Fig. 1B), a polysaccharide backbone composed of D-mannan and D-arabinan, and finally caps *(2,4,5)*. The structure of caps differs according to the species. Slow-growing mycobacteria, including *M. tuberculosis*; *Mycobacterium leprae*, the causative agent of leprosy; or *Mycobacterium bovis* BCG, the vaccine strain, possess LAMs capped with mannooligosaccharide units (ManLAMs) (Fig. 1C). Fast-growing mycobacteria, mainly opportunistic or nonpathogenic strains, have LAMs with either no caps (AraLAMs) or phospho-*myo*-inositol caps (PILAMs) (Fig. 1D). The type of capping is a major structural feature determining LAM immunomodulatory activities *(7)*. The main activities associated with ManLAMs are their ability to inhibit the activation of macrophages, the production of the Th1 proinflammatory cytokines interleukin-12 and tumor necrosis factor-α, *M. tuberculosis*–induced macrophage apoptosis, and the phagosome/lysosome fusion. All these activities are likely to favor the intramacrophagic survival of the bacilli. Thus, ManLAMs appear as virulence factors that contribute, via an immunosuppressive effect, to the persistence of slow-growing mycobacteria in the human reservoir. By contrast, PILAMs are able to induce the

release of a variety of proinflammatory cytokines through the activation of Toll-like 2 receptors. PILAMs are therefore likely to favor the killing of the fast-growing mycobacteria by activating the macrophages. No activity has been associated with AraLAMs so far.

The importance of LAM in the immunopathogenesis of tuberculosis has incited structural studies on LAM to first of all establish a precise structural model of the molecule and then to decipher the structure/function relationships. Structural studies on LAM are complicated by the size and the great heterogeneity of the molecule as well as by its amphipathic nature. The polysaccharidic core of LAM has been intensively studied, mainly by Brennan's group, using chemical or enzymatic degradations coupled to mass spectrometry (MS) and nuclear magnetic resonance (NMR) analyses *(2,8–10)*. In recent years, we have focused on the two domains essential for LAM activity: the MPI anchor and the caps. We review here the different procedures we have developed for the structural analysis of these domains.

Purification and Molecular Mass of LAM

A prerequisite for structural analysis is the obtaining of homogeneous fractions. Purification of LAM from the mycobacterial envelope is complicated by the presence of structurally related molecules such as the lipoglycan lipomannan (LM), the glycolipids phosphatidyl-*myo*-inositol-mannosides (PIM), or the glycans arabinomannan and mannan. Moreover, the difficulties encountered for purification of LAM are heightened by its intrinsic molecular heterogeneity (as described in this section). To obtain homogeneous fractions, the following critical steps are thus required:

1. Ethanol/water extraction of the lipoglycans from delipidated cells.
2. Enzymatic degradation of protein contaminants.
3. Separation of lipoglycans from glycans by hydrophobic interaction chromatography.
4. Size fractionation of lipoglycans by gel permeation chromatography.

Molecular mass is key structural information for determining the molecular architecture of molecules. LAMs migrate in sodium dodecyl sulfate-polyacrylamide gel electrophoresis (SDS-PAGE) as a broad unresolved band around 30 kDa according to protein size markers (Fig. 2A). LAM's precise molecular weight was determined for the first time in 1993 by matrix-assisted laser desorption/ionization-time of flight (MALDI-TOF)/MS *(11)*. The negative or positive MALDI mass spectra of LAM from *M. bovis* BCG (Fig. 2B) or *M. tuberculosis* exhibit a broad unresolved peak centered at *m/z* 17,000, assigned to molecular ions, indicating a mol wt of about 17 kDa for the major molecular species. The huge heterogeneity of LAM (±4 kDa) is highlighted by the linewidth of the peak (Fig. 2B). 2,5-Dihydroxybenzoic acid (DHB), solubilized in water/ethanol (1:1) was found to be the best matrix for LAM analysis. This matrix is indeed described to be convenient for oligosaccharide and glycolipids analysis *(12–14)*.

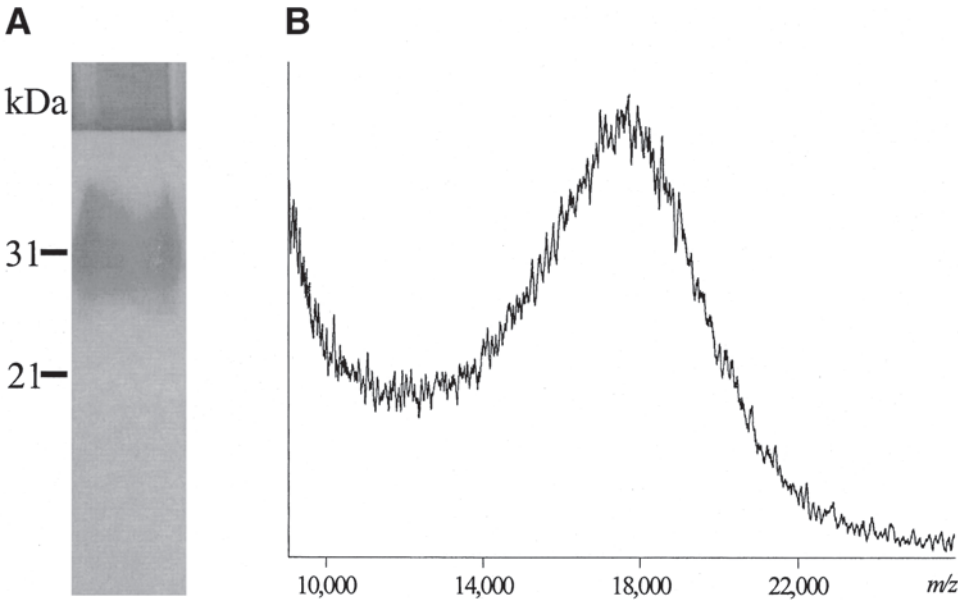

Fig. 2. **(A)** SDS-PAGE analysis and **(B)** negative MALDI mass spectrum of *M. bovis* BCG ManLAM. **(A)** ManLAM (5 µg) was run on a 15% polyacrylamide gel followed by silver nitrate staining. **(B)** A ManLAM solution (0.5 µL) at 10 µg/µL was mixed with 0.5 µL of the matrix solution (10 µg/µL of DHB in ethanol/water [1:1, v/v]) and analyzed by MALDI-TOF in the negative mode.

MPI Anchor

The anchor structure is based on an *sn*-glycero-3-phospho-(1-D-*myo*-inositol) unit with one α-D-Man*p* unit linked at O-2 of the *myo*-inositol. Additionally, the O-6 of *myo*-inositol unit is glycosylated by the mannan core (Fig. 1B). Four potential sites of acylation are present on the anchor: positions 1 and 2 of the glycerol unit, position 6 of the Man*p* unit linked at O-2 of *myo*-inositol, and position 3 of the *myo*-inositol *(15,16)* (Fig. 1B). LAMs are mainly acylated by palmitic and tuberculostearic acids and to a lesser extent by stearic acid. Routine gas chromatography (GC) analysis shows a mean of two to three fatty acids per ManLAM molecule in BCG or *M. tuberculosis (17,18)*. It is noticeable that the MPI anchor is shared by the LAM biosynthetic precursors, i.e., LM *(19)* and PIM *(15,19–21)*.

Acyl Groups on Glycerol

We first developed an analytical procedure to determine the structure of the acyl groups borne by the glycerol moiety of LAM *(17)*. LAMs are submitted to acetolysis (anhydrous acetic acid/acetic anhydride, 3:2 [v/v] at 110°C for 12 h), allowing cleavage between phosphate and glycerol but preserving the acyl-glycerol residues (Fig. 3) *(22)*. These residues, extracted by cyclohexane/water partition, are then analyzed by GC/MS in electron impact (EI) and CI/NH_3 ionization modes. Both mono-acyl-di-acetyl-

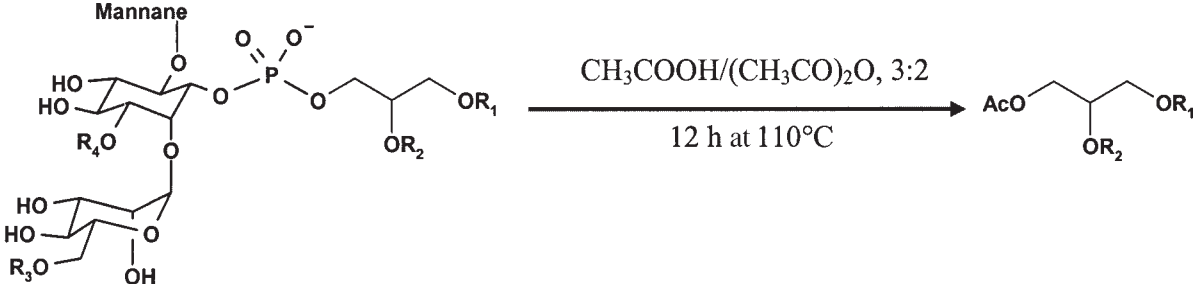

Fig. 3. Acetolysis of LAM. Three milligrams of LAM was treated with 400 µL of anhydrous acetic acid/acetic anhydride (3:2 [v/v]) at 110°C for 12 h. The reaction mixture was dried and vortexed with 400 µL of cyclohexane/water (1:1 [v/v]). The cyclohexane phase was analyzed by GC/MS in EI and CI modes.

sn-glycerol and di-acyl-mono-acetyl-*sn*-glycerol species are detected. 1,2-di-palmitoyl-3-acetyl-*sn*-glycerol, 1- or 2-palmitoyl-di-acetyl-*sn*-glycerol, 1- or 2-tuberculostearoyl-di-acetyl-*sn*-glycerol, and 1-tuberculostearoyl-2-palmitoyl-3-acetyl-*sn*-glycerol are detected in *M. bovis* BCG and *M. tuberculosis (17,18)*. These data first revealed the heterogeneity of the MPI anchor because at least four molecular species were identified that differ in palmitic and tuberculostearic acid composition and location.

This strategy has been successfully applied to the MPI anchor analysis of LM *(19)* and PIM *(20,21)*. In the case of PIM, this strategy provides more structural information because both the acyl-glycerol and acyl-phospho-*myo*-inositol-mannoside moieties can be analyzed by electrospray ionization (ESI)/MS or MALDI/MS. Thus, the nature of the fatty acids present on *myo*-inositol and/or mannose units can be identified *(20,21)*.

Characterization of LAM Acyl-Forms by ^{31}P NMR

The phosphorous atom can be used as a gate to enter into the MPI anchor. Thus, to characterize further the heterogeneity of the MPI anchor, we have developed one-dimensional (1D) ^{31}P and two-dimensional (2D) ^{1}H-^{31}P NMR approaches.

The 1D ^{31}P spectrum of multiacylated LAM recorded in D_2O exhibits a broad unresolved signal with a width of 150 Hz *(16,17)* (Fig. 4A). This is owing to the fact that LAMs are amphipathic 17-kDa macromolecules characterized by a hydrophobic MPI anchor and a hydrophilic carbohydrate domain. This asymmetry in polarity leads to the formation of aggregates in water. Therefore, the motion of LAM in solution thus tends to be much slower than expected from the molecular weight of a single molecule. This means that the overall rotational correlation times τ_c are much larger than expected, and the NMR transverse relaxation time T_2 tends to be small, leading to line broadening *(23)*.

To improve the resolution of the 1D ^{31}P NMR spectra of LAMs, we have tested two different solubilization procedures *(16)*. LAMs were first tentatively dissolved in water with the aid of detergents *(24)*, which proved to be inadequate. Indeed, no ^{31}P signal was obtained in 1D ^{31}P experiments carried out in the presence of Triton X-114 or Triton X-100. Solubilization with sodium deoxycholate (DOC) (1%), which has been found to solubilize phospholipids in water and to improve the resolution of 1D ^{31}P NMR spectra *(25,26)*, allowed the recording of two well-separated fine ^{31}P resonances, but 2D data were not recordable. An increase in the DOC-to-LAM ratio was expected to improve the 1D ^{31}P spectra *(27,28)*; however, the resulting mixture was a gel at room temperature and was unsuitable for NMR analysis. A second approach consisted of solubilizing LAM in organic solvents. DMSO-d6 was found to give the best results *(16)*. Four to five separated resonances were observed for *M. bovis* BCG *(16)* (Fig. 4B) or *M. tuberculosis* LAM *(5,18)* and provided well-defined correlations in 2D experiments. Temperature was also shown to have a marked influence. At 303 K, phosphorus resonates as a broad unresolved signal, whereas at 323 K the signals

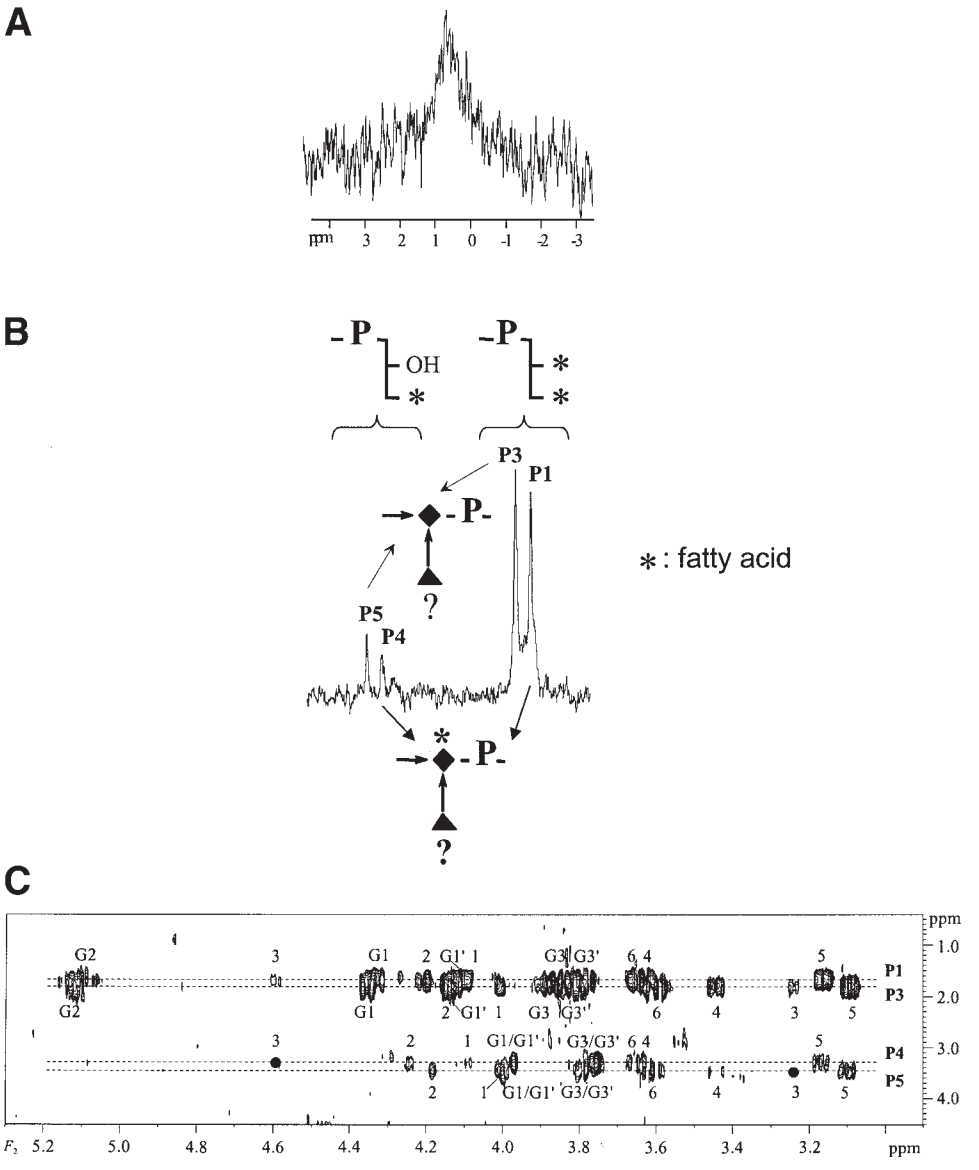

Fig. 4. ^{31}P NMR analysis of *M. bovis* BCG ManLAM. **(A)** 1D ^{31}P spectrum of in D_2O at 313 K. ManLAM concentration was 120 mg/mL, 512 ns. **(B)** 1D ^{31}P spectrum in DMSO-d6 at 343 K. ManLAM concentration was 54 mg/mL, 1662 ns. Phosphates P1 and P3 characterize an anchor bearing a diacylated glycerol, the *myo*-inositol unit being acylated in the case of P1. Phosphates P4 and P5 typify an anchor with a 1-acyl-2-lyso-glycerol unit, the *myo*-inositol unit being acylated in P4. Asterisks correspond to fatty acyl appendages; P, phosphate; ◆, *myo*-inositol; ▲, α-Man*p*; ?, acylation state not determined. **(C)** 2D ^{1}H-^{31}P HMQC-HOHAHA spectrum τ_m 53 ms in DMSO-d6 at 343 K. Numerals correspond to the proton number of the *myo*-inositol units, and numerals with the letter *G* correspond to the proton number of the glycerol units. ●, Connectivities present on spectra but with weak intensity.

are well separated with an increase in the signal-to-noise ratio at 343 K. DMSO-d6 thus appeared to be an efficient solvent system for ^{31}P NMR analysis of ManLAM, enabling separation of phosphate resonances poorly resolved in D_2O (linewidth of 9–16 Hz in DMSO-d6 vs 150–200 Hz in D_2O) *(16)* (Fig. 4B) and the recording of 2D ^{1}H-^{31}P HMQC-HOHAHA experiments *(29)* (Fig. 4C). The 2D ^{1}H-^{31}P HMQC-HOHAHA spectrum provides a set of correlations between the different phosphate resonances and the protons of the units by which the phosphates are esterified (Fig. 4C). Then, the degree of acylation of glycerol and *myo*-Ins units can be deduced from the chemical shift values. Attribution of the different resonances was facilitated by analysis of the LAM biosynthetic precursors PIM that show the same acylation sites but are smaller molecules and therefore can be fully analyzed by NMR *(19)*. It is noteworthy that ^{31}P analysis of PIMs can be performed after their solubilization in chloroform/methanol/water.

The different phosphate evidenced by the ^{31}P individual resonances belong to phosphatidylinositol units differing in structure and particularly in the number and position of fatty acid substituents (Fig. 4B). Phosphates P1 and P3 characterize an anchor bearing a diacylated glycerol, the *myo*-inositol unit being acylated in the case of P1. Phosphates P4 and P5 typify an anchor with a 1-acyl-2-lyso-glycerol unit, the *myo*-inositol unit being acylated in P4 *(16,19)*. The number of fatty acids on the glycerol has a greater effect on the ^{31}P chemical shift than that of the fatty acids on the *myo*-inositol. For example, the presence of a second fatty acid on the glycerol led to an upfield shift of 1.7 ppm, whereas on the *myo*-inositol a fatty acid shifted the ^{31}P signal upfield only by 0.17 ppm. Unfortunately, our analytical approach does not allow determination of the acylation state of the Man*p* units. However, it allowed us to demonstrate, for the first time, a new site of acylation on the family of mycobacterial lipoglycans (PIMs, LMs, LAMs), i.e., position 3 of the *myo*-inositol unit *(16,18,19)*.

This nondestructive approach allows structural studies of the native multiacylated MPI anchor, whereas earlier studies on LAM had mainly been conducted on alkali-treated molecules, owing to the amphipathic nature of the native molecules and the difficulties encountered for their solubilization. This approach has been successfully applied for characterization of the MPI anchor acyl-forms in various LAM *(16,18,30,31)*, LM *(19)*, PIM *(19–21)*, or LAM-like molecules *(32,33)*.

Caps

Two types of capping motifs have been identified. Mannooligosaccharide units cap the LAM from slow-growing mycobacteria *(9,11)*, whereas phosphoinositide units cap the LAM from fast-growing mycobacteria, *Mycobacterium smegmatis* and *Mycobacterium fortuitum (34)*. The mannose caps consist of mono-, (α1→2)-di-, and (α1→2)-tri-mannosyl units *(9)* (Fig. 1C), and the phosphoinositide caps consist of *myo*-inositol-1-phosphate esterifying some β-D-Ara*f* units at O-5 *(34–36)* (Fig. 1D).

Phosphoinositide Caps

The structure of phosphoinositide caps has been investigated by 1D ^{31}P and 2D ^{1}H-^{31}P HMQC-HOHAHA NMR. Indeed, the phosphorus of phosphoinositide caps exhibits a ^{31}P resonance that is distinct from those of the phosphorus of the MPI anchor *(34)*. Thus, the 2D ^{1}H-^{31}P HMQC-HOHAHA spectrum allows, in a single step, one to investigate the structure of the MPI acyl-forms and also the presence of phosphoinositide caps. Moreover, it demonstrates that the phosphate of the caps was esterified by a *myo*-inositol unit at its O-1 or by a β-D-Ara*f* unit at its O-5 *(34)*. The number of phosphoinositide caps present per PILAM molecule can be determined by relative integration of the ^{31}P signals, when one knows that LAMs contain a single phosphorus atom in the MPI anchor. It is noteworthy that poorly acylated LAMs can be directly analyzed in water *(34)*, whereas, as for the MPI anchor, multiacylated LAMs have to be solubilized in dimethyl sulfoxide (DMSO). So far phosphoinositide caps have been found in LAMs from *M. smegmatis (34)* and *M. fortuitum* (unpublished data).

Mannose Caps

Mannose caps are the epitopes of ManLAM recognized by its host receptors, the C-type lectins, mannose receptor *(37)*, DC-SIGN *(38)*, mannose-binding protein *(39)*, and surfactant proteins A *(40)* and D *(41)*. The structure of the different mannooligosaccharide caps and their number per molecule are key parameters for enabling a fuller understanding of ManLAM recognition by C-type lectins *(42)*.

We have developed an analytical approach, based on capillary electrophoresis coupled to laser-induced fluorescence detection (CE-LIF), that allows determination of the number of each type of cap motif per ManLAM molecule as well as their glycosidic linkages *(42)*. The quantification of caps is based on three steps: (1) accurate determination of ManLAM concentration by CE-LIF, (2) recovery of the mannooligosaccharide caps following mild acid hydrolysis of ManLAM in the presence of an internal standard, and (3) absolute quantification of each type of mannooligosaccharide cap by CE-LIF.

The accurate concentration of ManLAM is calculated from the molecular weight of ManLAM determined by MALDI/MS (Fig. 2B) and from the quantification by CE-LIF of arabinose (Ara) and mannose (Man) released after total acid hydrolysis (2*M* TFA, 2 h at 110°C) in the presence of mannoheptose as internal standard. LAM is exclusively composed of neutral monosaccharides that do not significantly absorb ultraviolet light. Hydrolysis reaction products are thus submitted to 1-aminopyrene-3,6,8-trisulfonate (APTS) tagging by reductive amination *(43)* (Fig. 5A), allowing in a single step of derivatization the introduction of negative charges on the neutral mannooligosaccharide caps and a chromophore for high-sensitivity LIF detection. Derivatization products are then submitted to CE-LIF separation with the cathode on the injection side and the anode on the

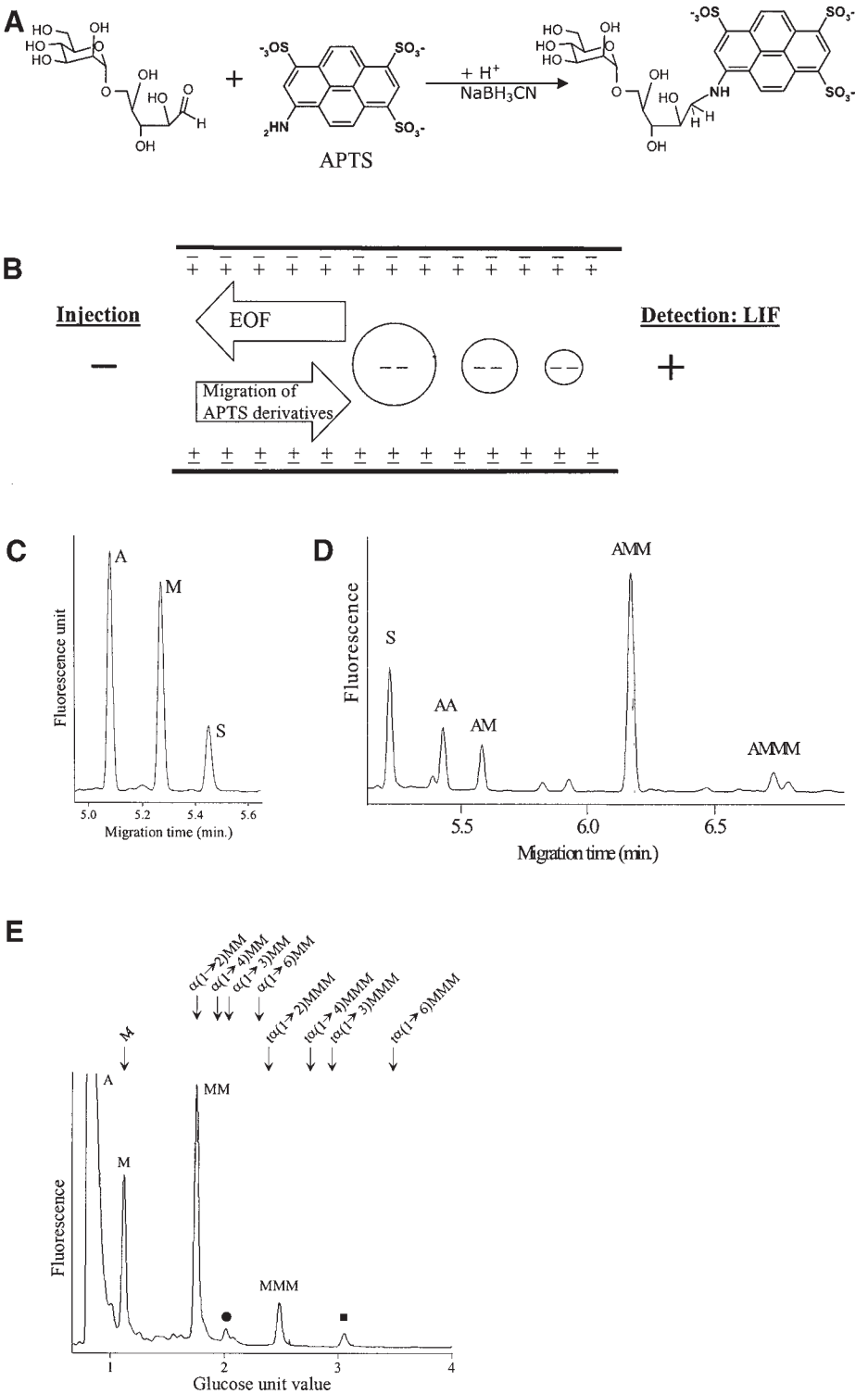
A
APTS
+ H+
NaBH3CN
B
Injection
EOF
Migration of
APTS derivatives
Detection: LIF
C
A
M
S
Fluorescence unit
Migration time (min.)
D
AMM
S
AA
AM
AMMM
Fluorescence
Migration time (min.)
E
α(1→2)MM
α(1→4)MM
α(1→3)MM
α(1→6)MM
α(1→2)MMM
α(1→4)MMM
α(1→3)MMM
α(1→6)MMM
M
A
MM
M
MMM
Fluorescence
Glucose unit value

Fig. 5.

detection side (reverse polarity) (Fig. 5B). Analyses are carried out at 25°C with an applied voltage of 20 kV, using an uncoated fused-silica capillary column and 1% (w/v) acetic acid, 30 m*M* triethylamine in water, pH 3.5, as running electrolyte. The use of low pH suppresses ionization of the capillary surface silanol groups, leading to a value for electroendosmotic flow of about zero *(44)*. Under these conditions, the secondary amino group carries a positive charge, leading to an overall of two negative charges that provide the driving force for electrophoretic mobility of derivatized mono- or oligosaccharides. Triethylamine has been found to increase separation reproductibility by masking the interaction between the labeled carbohydrates and the inner surface of the silica capillary *(45,46)*. Since only one chromophore is present per derivatized molecule (Fig. 5A), peak integration directly provides the molar ratios Ara/mannoheptose and Man/mannoheptose (Fig. 5C), which allows determination of the concentration by weight (in µg/µL) of the ManLAM solutions. From the average molecular weight of ManLAM, determined by MALDI/MS, an average ManLAM molarity is obtained and used for cap quantification.

The mannooligosaccharide caps are released by mild acid hydrolysis (0.1*N* HCl, 20 min at 110°C) of ManLAM that cleaves the arabinofuranosidic bonds of the arabinan domain but preserves the mannopyranosidic bonds

---

Fig. 5. *(opposite page)* CE-LIF analysis of ManLAM. **(A)** APTS derivatization reaction. Dried reaction products were mixed with 0.3 µL of 0.2 *M* APTS in 15% acetic acid and 0.3 µL of a 1 *M* sodium cyanoborohydride solution dissolved in tetrahydrofuran *(43)*. The reaction was performed for 90 min at 55°C. **(B)** CE separation of APTS derivatives. Analyses were performed on a P/ACE capillary electrophoresis system (Beckman) with the cathode on the injection side and the anode on the detection side (reverse polarity). APTS derivatives were loaded by applying a 0.5-psi (3.45-kPa) vacuum for 5 s (6.5 nL injected). Separations were performed in the reverse mode using an uncoated fused-silica capillary column of 50-µm id with a 40-cm effective length. The detection system consisted of a Beckman LIF equipped with a 4-mW argon-ion laser with an excitation wavelength of 488 nm and emission wavelength filter of 520 nm. **(C)** CE analysis of total acid hydrolyzed *M. bovis* BCG ManLAM. One microgram of lipoglycan and 1 nmol of mannoheptose were hydrolyzed using 30 µL of 2 *M* TFA for 2 h at 110°C, dried, APTS derivatized, and subjected to CE-LIF as in **B**. A, Ara-APTS; M, Man-APTS; S, internal standard, mannoheptose-APTS. **(D)** CE analysis of mild acid hydrolyzed *M. bovis* BCG ManLAM. One microgram of lipoglycan and 0.1 nmol of mannoheptose were hydrolyzed with 15 µL of 0.1 *M* HCl for 20 min at 110°C, dried, and APTS derivatized and subjected to CE-LIF as in **B**. S, internal standard, mannoheptose-APTS; AA, Ara*f*-α(1→5)-Ara-APTS; AM, Man*p*-Ara-APTS; AMM, Man*p*-Man*p*-Ara-APTS; AMMM, Man*p*-Man*p*-Man*p*-Ara-APTS. **(E)** CE analysis of acetolyzed *M. tuberculosis* H37Ra ManLAM. Mannooligosaccharide caps from 10 g of ManLAM were recovered after dialysis and then acetolyzed with 15 µL of an acetic anhydride/acetic acid/sulfuric acid (10:10:1 [v/v/v]) mixture for 3 h at 40°C. Acetolysis products were deacetylated with 20 µL of a methanol/20% aqueous ammonia solution (1:1 [v/v]) at 37°C for 18 h. The samples were then submitted to APTS tagging and CE-LIF migration as in **B**. A, Ara-APTS; M, Man-APTS; MM, Man-Man-APTS; MMM, Man-Man-Man-APTS. Peaks labeled with ● and ■ correspond to Man*p*-Ara-APTS and Man*p*-Man*p*-Ara-APTS, respectively, owing to a noncomplete removal of the Ara unit by the acetolysis reaction.

of the caps *(11)*. Caps are thus released with an arabinosyl unit at their reducing end (Figs. 1C, 5A). To quantify the absolute amount of mannooligosaccharide motifs per ManLAM molecule, precise amounts of ManLAM, determined as described above, with mannoheptose as internal standard are submitted to mild acid hydrolysis, APTS tagging, and CE-LIF analysis (Fig. 5D). The different peaks have been assigned by coinjection with standards, by CE coupled to ESI/MS *(47)*, or after collecting the corresponding compounds and their analysis by MALDI-TOF/MS *(48)*. The amount of each cap motif, mono- (AM), di- (AMM), or trimannosyl (AMMM) units, per ManLAM molecule is determined relative to the internal standard (S) (Fig. 5D) *(42)*. This approach has been successfully applied for investigation of the presence of caps and their quantification in various LAM *(17,18,30,31,42)* or LAM-like molecules *(32,33,49)* as well as for the monitoring of enzymatic degradation of ManLAM *(30,38,40)*.

We have also developed a CE-LIF approach to elucidate the type of glycosidic linkage of the cap units *(42)*. CE is able to separate dimannoside-APTS units differing only by the type of glycosidic linkage (Fig. 5E). Indeed, CE separation of carbohydrate APTS derivatives is based on the hydrodynamic volume-to-charge ratios, rather than on the mass-to-charge ratios *(50–52)*. The mannooligosaccharide caps obtained by mild acid hydrolysis of ManLAM are isolated by dialysis and then submitted to acetolysis in order to cleave the arabinosyl unit still attached to the oligomannosyl moiety *(42)*. The resulting dimannosyl unit in *M. bovis* BCG or *M. tuberculosis* ManLAM, after APTS derivatization, unambiguously coelutes with the α-D-Man*p*-(1→2)-D-Man-APTS standard (Fig. 5E) in agreement with the previously proposed structure *(9)*. Owing to the lack of commercial trimannoside standards differing by their glycosidic linkages, this analytical approach cannot be directly applied for cap trimannoside characterization. However, it has been demonstrated that the electrophoretic mobility of maltooligosaccharide derivatives is a linear function of the degree of polymerization *(45)*. The trimannoside-APTS derivative shows an experimental electrophoretic mobility of 2.48 glucose units (GU), close to the theoretical one of 2.39 GU calculated for an α(1→2)-trimannoside from the electrophoretic mobilities of α-D-Man*p* at 1.11 GU and of α-D-Man*p*-(1→2)-D-Man at 1.75 GU (Fig. 5E). The theoretical and experimental values are slightly different owing to the fact that the relation between the migration time and the degree of polymerization is not strictly linear for a degree of polymerization lower than five *(45)*. The results confirm the unique α(1→2) linkage for the mannooligosaccharide caps of *M. bovis* BCG and *M. tuberculosis* ManLAM. With this method, interglycosidic linkages can be investigated at the subnanomole level thanks to LIF detection. Moreover, multiple steps of chemical modification are not necessary, as in the alditol acetate procedure *(42)*.

One significant aspect of these methods using CE-LIF is their capacity to quantify each type of mannooligosaccharide cap per ManLAM molecule and to determine their glycosidic linkage from <1 nmol of ManLAM. CE

clearly emerges as a useful tool for structural analysis of lipoglycans, either intact or as their carbohydrate parts (for a review *see* ref. *53*).

Conclusion

The basic structural features of LAM are now established and the global structure of the different domains has been precisely determined. The structural data available so far allow a thorough understanding of LAM structure/function relationships. Nevertheless, structural analysis of LAM now faces two main challenges. One is the identification of low abundant motifs, present in very small numbers per molecule, but likely to be responsible for some LAM activities. The other challenge is the structural analysis of LAM from mycobacteria directly isolated from the host, without any in vitro cultures. Indeed, the structure of LAM from mycobacteria grown in vivo may differ from that observed in vitro, and this is likely to again affect any LAM-associated biologic functions.

These two challenges will require considerable effort and the development of sophisticated structural analysis strategies such as ^{13}C enrichment of the LAM molecule for NMR analysis or high-resolution MS such as Fourier transform ion cyclotron resonance MS for identification of the low abundant motifs *(54)*. Structural analysis of LAM from mycobacteria grown in vivo will allow investigation of the LAM structure from a few milligrams of mycobacteria. This will require the development of efficient purification protocols and highly sensitive analytical procedures. Whereas NMR will not be a suitable technique owing to the lack of sensitivity, CE-LIF appears to be a method of choice for such analyses. The CE-LIF strategies reviewed in this article provide the sensitivity required for analysis of the carbohydrate part of LAM, including the caps, and have been applied to the comparative structural analysis of LAM from *M. avium* grown either in vitro or in mice (unpublished results) *(55)*.

Acknowledgments

We gratefully acknowledge Kevin J. C. Gibson (University of Birmingham, UK) for checking the translation of the manuscript into English.

References

1 Brennan, P. J. and Nikaido, H. (1995), *Annu. Rev. Biochem.* **64,** 29–63.
2 Chatterjee, D. and Khoo, K. H. (1998), *Glycobiology* **8,** 113–120.
3 Vercellone, A., Nigou, J., and Puzo, G. (1998), *Front. Biosci.* **3,** e149–e163.
4. Gilleron, M., Rivière, M., and Puzo, G. (2001) in *Glycans in Cell Interaction and Recognition: Therapeutic Aspects*, Aubery, M., ed., Harwood Academic, Amsterdam, pp. 113–140.
5 Nigou, J., Gilleron, M., and Puzo, G. (2003), *Biochimie* **85,** 153–166.
6. Brennan, P. J. (2003), *Tuberculosis (Edinb.)* **83,** 91–97.
7 Nigou, J., Gilleron, M., Rojas, M., Garcia, L. F., Thurnher, M., and Puzo, G. (2002), *Microbes Infect.* **4,** 945–953.

8 Chatterjee, D., Bozic, C. M., McNeil, M., and Brennan, P. J. (1991), *J. Biol. Chem.* **266,** 9652–9660.
9 Chatterjee, D., Lowell, K., Rivoire, B., McNeil, M. R., and Brennan, P. J. (1992), *J. Biol. Chem.* **267,** 6234–6239.
10 Chatterjee, D., Khoo, K. H., McNeil, M. R., Dell, A., Morris, H. R., and Brennan, P. J. (1993), *Glycobiology* **3,** 497–506.
11. Venisse, A., Berjeaud, J. M., Chaurand, P., Gilleron, M., and Puzo, G. (1993), *J. Biol. Chem.* **268,** 12,401–12,411.
12 Mock, K. K., Davey, M., and Cottrell, J. S. (1991), *Biochem. Biophys. Res. Commun.* **177,** 644–651.
13. Stahl, B., Steup, M., Karas, M., and Hillenkamp, F. (1991), *Biochem. Biophys. Res. Commun.* **63,** 1463–1466.
14. Egge, H., Peter-Katalini, J., Karas, M., and Stahl, B. (1991), *Pure Appl. Chem.* **63,** 491–498.
15 Khoo, K. H., Dell, A., Morris, H. R., Brennan, P. J., and Chatterjee, D. (1995), *Glycobiology* **5,** 117–127.
16 Nigou, J., Gilleron, M., and Puzo, G. (1999), *Biochem. J.* **337,** 453–460.
17 Nigou, J., Gilleron, M., Cahuzac, B., Bounery, J. D., Herold, M., Thurnher, M., and Puzo, G. (1997), *J. Biol. Chem.* **272,** 23,094–23,103.
18 Gilleron, M., Bala, L., Brando, T., Vercellone, A., and Puzo, G. (2000), *J. Biol. Chem.* **275,** 677–684.
19 Gilleron, M., Nigou, J., Cahuzac, B., and Puzo, G. (1999), *J. Mol. Biol.* **285,** 2147–2160.
20 Gilleron, M., Ronet, C., Mempel, M., Monsarrat, B., Gachelin, G., and Puzo, G. (2001), *J. Biol. Chem.* **276,** 34,896–34,904.
21 Gilleron, M., Quesniaux, V. F., and Puzo, G. (2003), *J. Biol. Chem.* **278,** 29,880–29,889.
22 Ferguson, M. A., Haldar, K., and Cross, G. A. (1985), *J. Biol. Chem.* **260,** 4963–4968.
23 Wang, Y. and Hollingsworth, R. I. (1995), *Anal. Biochem.* **225,** 242–251.
24 Roberts, M. F., Adamich, M., Robson, R. J., and Dennis, E. A. (1979), *Biochemistry* **18,** 3301–3308.
25 Batley, M., Packer, N. H., and Redmond, J. W. (1985), *Biochim. Biophys. Acta* **821,** 179–194.
26. Masoud, H., Altman, E., Richards, J. C., and Lam, J. S. (1994), *Biochemistry* **33,** 10,568–10,578.
27. Denis, E. A. and Plücktun, A. (1984), in *Phosphorus-31NMR—Principles and Applications*, Gorenstein, D. G., ed., Academic, Orlando, FL, pp. 423–446.
28 Rosner, M. R., Khorana, H. G., and Satterthwait, A. C. (1979), *J. Biol. Chem.* **254,** 5818–5825.
29. Lerner, L. and Bax, A. (1986), *J. Magn. Reson.* **69,** 375–380.
30 Nigou, J., Zelle-Rieser, C., Gilleron, M., Thurnher, M., and Puzo, G. (2001), *J. Immunol.* **166,** 7477–7485.
31 Ludwiczak, P., Gilleron, M., Bordat, Y., Martin, C., Gicquel, B., and Puzo, G. (2002), *Microbiology* **148,** 3029–3037.
32 Garton, N. J., Gilleron, M., Brando, T., Dan, H. H., Giguere, S., Puzo, G., Prescott, J. F., and Sutcliffe, I. C. (2002), *J. Biol. Chem.* **277,** 31,722–31,733.
33 Gibson, K. J., Gilleron, M., Constant, P., Puzo, G., Nigou, J., and Besra, G. S. (2003), *Biochem. J.* **372,** 821–829.
34 Gilleron, M., Himoudi, N., Adam, O., Constant, P., Venisse, A., Riviere, M., and Puzo, G. (1997), *J. Biol. Chem.* **272,** 117–124.
35. Khoo, K. H., Dell, A., Morris, H. R., Brennan, P. J., and Chatterjee, D. (1995), *J. Biol. Chem.* **270,** 12,380–12,389.
36. Désiré, J. and Prandi, J. (1999), *Carbohydr. Res.* **317,** 110–118.
37 Schlesinger, L. S., Hull, S. R., and Kaufman, T. M. (1994), *J. Immunol.* **152,** 4070–4079.
38 Maeda, N., Nigou, J., Herrmann, J. L., Jackson, M., Amara, A., Lagrange, P. H., Puzo, G., Gicquel, B., and Neyrolles, O. (2002), *J. Biol. Chem.* **278,** 5513–5516.
39 Polotsky, V. Y., Belisle, J. T., Mikusova, K., Ezekowitz, R. A., and Joiner, K. A. (1997), *J. Infect. Dis.* **175,** 1159–1168.

40 Sidobre, S., Nigou, J., Puzo, G., and Riviere, M. (2000), *J. Biol. Chem.* **275,** 2415–2422.
41 Ferguson, J. S., Voelker, D. R., McCormack, F. X., and Schlesinger, L. S. (1999), *J. Immunol.* **163,** 312–321.
42 Nigou, J., Vercellone, A., and Puzo, G. (2000), *J. Mol. Biol.* **299,** 1353–1362.
43 Guttman, A., Chen, F. T., Evangelista, R. A., and Cooke, N. (1996), *Anal. Biochem.* **233,** 234–242.
44 Oefner, P. J. and Chiesa, C. (1994), *Glycobiology* **4,** 397–412.
45 Chiesa, C. and Horvath, C. (1993), *J. Chromatogr.* **645,** 337–352.
46 Chiesa, C. and O'Neill, R. A. (1994), *Electrophoresis* **15,** 1132–1140.
47 Monsarrat, B., Brando, T., Condouret, P., Nigou, J., and Puzo, G. (1999), *Glycobiology* **9,** 335–342.
48 Ludwiczak, P., Brando, T., Monsarrat, B., and Puzo, G. (2001), *Anal. Chem.* **73,** 2323–2330.
49 Gibson, K. J., Gilleron, M., Constant, P., Puzo, G., Nigou, J., and Besra, G. S. (2003), *Microbiology* **149,** 1437–1445.
50 Chen, F. T. and Evangelista, R. A. (1995), *Anal. Biochem.* **230,** 273–280.
51 Guttman, A. and Herrick, S. (1996), *Anal. Biochem.* **235,** 236–239.
52 Guttman, A. and Pritchett, T. (1995), *Electrophoresis* **16,** 1906–1911.
53 Lamari, F. N., Gioldassi, X. M., Mitropoulou, T. N., and Karamanos, N. K. (2002), *Biomed. Chromatogr.* **16,** 116–126.
54 Treumann, A., Xidong, F., McDonnell, L., Derrick, P. J., Ashcroft, A. E., Chatterjee, D., and Homans, S. W. (2002), *J. Mol. Biol.* **316,** 89–100.
55. Ludwiczak, P. (2002), PhD thesis, Université Paul Sabatier, Toulouse, France.